The behavior of cold-curing resin after thermal and UV radiation exposures

Jaroslav Hornak ✉; Pavel Trnka; Pavel Prosr; ... et. al

Check for updates

View Online   Export Citation   CrossMark

Articles You May Be Interested In

Effect of MgO nanoparticles on material properties of cold-curing epoxy and polyurethane mixtures

AIP Conference Proceedings (November 2021)

Effect of ZnO nanoparticles on the dielectric properties of polyurethane and epoxy resins

AIP Conference Proceedings (November 2021)

Influence of prolonged mixing of silicon dioxide nanoparticles on the electrical properties of resin nanocomposites

AIP Conference Proceedings (May 2023)

The Behavior of Cold-Curing Resin after Thermal and UV Radiation Exposures

Jaroslav Hornak[1, a)], Pavel Trnka[1], Pavel Prosr[1], Ondrej Michal[1] and Jiri Kopriva[1]

[1]*Department of Materials and Technology, Faculty of Electrical Engineering, University of West Bohemia, Pilsen, Czech Republic*

a) *Corresponding author: jhornak@fel.zcu.cz*

Abstract. Potting compounds are widely used in electrical engineering. One of the distinctive subgroups is the so-called cold-cure potting compounds. These potting compounds are mainly used for mechanical or photosensitive protection and are thus often exposed to extreme conditions due to their nature of use. The epoxy mixture was subjected to a separate degradation process of elevated temperature (180 °C) and UV-B radiation (peak at 302 nm, 3x20 W) for 500 h. Electrical (volume resistivity, space charge, relative permittivity, dielectric losses), mechanical (tensile strength) and optical (FTIR) methods were used to verify the degree of degradation. From the presented results it can be seen that in terms of volume resistivity there is only a minimal decrease in both cases. However, the change in dielectric behavior is evident in the relative permittivity and loss factor, especially after the glass transition temperature is exceeded in the case of thermally aged material. The different behavior is also observable in terms of space charge trapping and de-trapping. Mechanical tests showed a significant decrease in tensile strength for the thermally aged material (≥ 50 % decrease). There was also a negative change in the case of UV-B exposure, but not as pronounced (≥ 10 % decrease). The thermal oxidation and photooxidation were confirmed by presence of additional spectral bands at 1740 cm^{-1} and 1650 cm^{-1}, respectively. These phenomena also resulted in typical discoloration of the samples (temperature: browning, UV-B: yellowing) after the exposure.

INTRODUCTION

Epoxy resins (ER), along with polyurethanes (PU), unsaturated polyesters (UP), phenolic resins (PR), and amine resins (AR), represent an important group of synthetic thermosets that are used in many industrial applications, such as automotive, electrical and mechanical engineering, civil engineering, building engineering packaging, etc. [1]. This wide range of applications of ERs is mainly due to their good adhesion to various materials, but also due to their superior mechanical, chemical and electrical properties [2]. However, their application, especially in exteriors, may be limited due to lower UV stability [3]. Another limiting problem can arise because most ERs are cured in the presence of elevated temperatures for a relatively long time (several hours). And whereas electronic devices may involve components that are temperature sensitive, it is necessary to use cold-curing ERs [4]. These ERs are cured at normal temperatures by reacting the base compound with a hardener without any additional heating. This process can be accelerated by applying a higher temperature (Fig.1 (a)), but this is not strictly necessary. Since aliphatic amines or polyamines [5] are used as hardeners, there is a significant limitation in terms of glass transition temperature (around 60 °C), which must always be considered before the application. The expected reactivity of resin and amine hardener is shown in Fig. 1 (b). The process of curing reaction of cold-cure ERs can be divided into three basic phases: (i) open time, (ii) initial cure phase, and (iii) final cure phase.

- **Open Time -** This phase is also called working time or wet lay-up time [6]. It is part of the curing time after mixing of base material with hardener and means that the epoxy mixture remains fluid and processable.
- **Initial cure phase** - The epoxy enters the initial curing phase when it begins to gel. The epoxy is no longer workable and will be transitioning from a sticky gel consistency to the strength of a hard material (depending on the nature of the resin).
- **Final cure phase** - Mixture of epoxy resin and hardener are cured to a solid state. At this point, the epoxy has reached most of its ultimate strength.
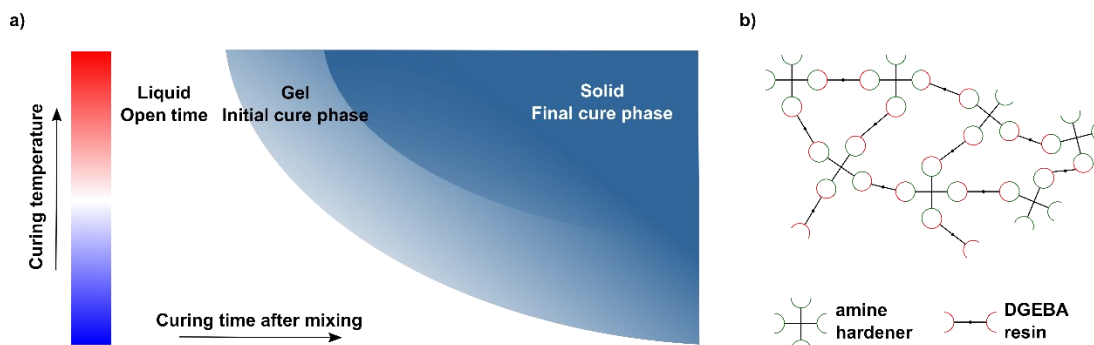

FIGURE 1. Curing of epoxy resin: a) effects of temperature on curing time and on the resin state; b) expected reactivity of DGEBA and amine hardener (redrawn and adapted from: [7-8]).

EXPERIMENTAL DETAILS

Materials and Exposures

The base material (Bisphenol A) was vacuumed for 1 hour to remove air bubbles formed during transfer to laboratory glass bottles. The amine hardener in the recommended ratio (1:0.45) was then applied and incorporated into the base material by mechanical mixing (700 rpm for 5 minutes). The mixture was again vacuumed for 10 minutes with a very slow stirring speed (50 rpm). Finally, the finished mixture has been poured into flat square-shaped molds with dimensions $100 \times 100 \times 1.0 \pm 0.2$ mm. Then the samples were cured at laboratory conditions (23 ± 2 °C, $53\pm5\%$ RH) minimal for 48 h. Each set of prepared samples included 5 flat samples and 10 dog-bone samples.

Temperature exposure of the samples was carried out in a laboratory oven (SF75 Plus, Memmert) for 500 h at 180 °C. This temperature is high enough to cause irreversible changes in the structure of the material in such a relatively short time. The UV-B exposure was carried out in a self-constructed box equipped with a UV source consisting of three 20 W fluorescent tubes (TL20W/12 RS SLV/25, Philips). These lamps generate UV-B radiation mainly in the wavelength range from 290 nm to 315 nm with a peak power at 302 nm. Exposure to UV-B radiation was carried out for 500 hours. Individual test samples are further marked in the text and graphs as (i) initial state (EP - IS), (ii) UV-B exposure (EP - UV), and (iii) thermal exposure (EP - T).

Methods, Results and Discussions

Dissipation Factor and Relative Permittivity Measurement

The relative permittivity and dissipation factor were investigated using broadband dielectric spectroscopy (Alpha-A, Novocontrol Technologies) and vector bridge (2830/2831, Tettex) measurement devices. These are the basic electrical parameters characterizing the behavior of a dielectric material in an alternating electric field. These methods were chosen mainly because broadband spectroscopy characterizes the material at a voltage of 1 V_{RMS} with a variable frequency (from 0.5 Hz to 1 MHz), whereas the vector bridge measurement takes place at a voltage of 1000 V_{RMS} at a constant frequency (50 Hz). Frequency dependence measurements were performed at room

temperature (23±2 °C). The temperature dependence of the behavior of the investigated materials was realized on a vector bridge in the temperature range from 30 to 80 °C. The measurement results (average) are shown in Fig. 2.
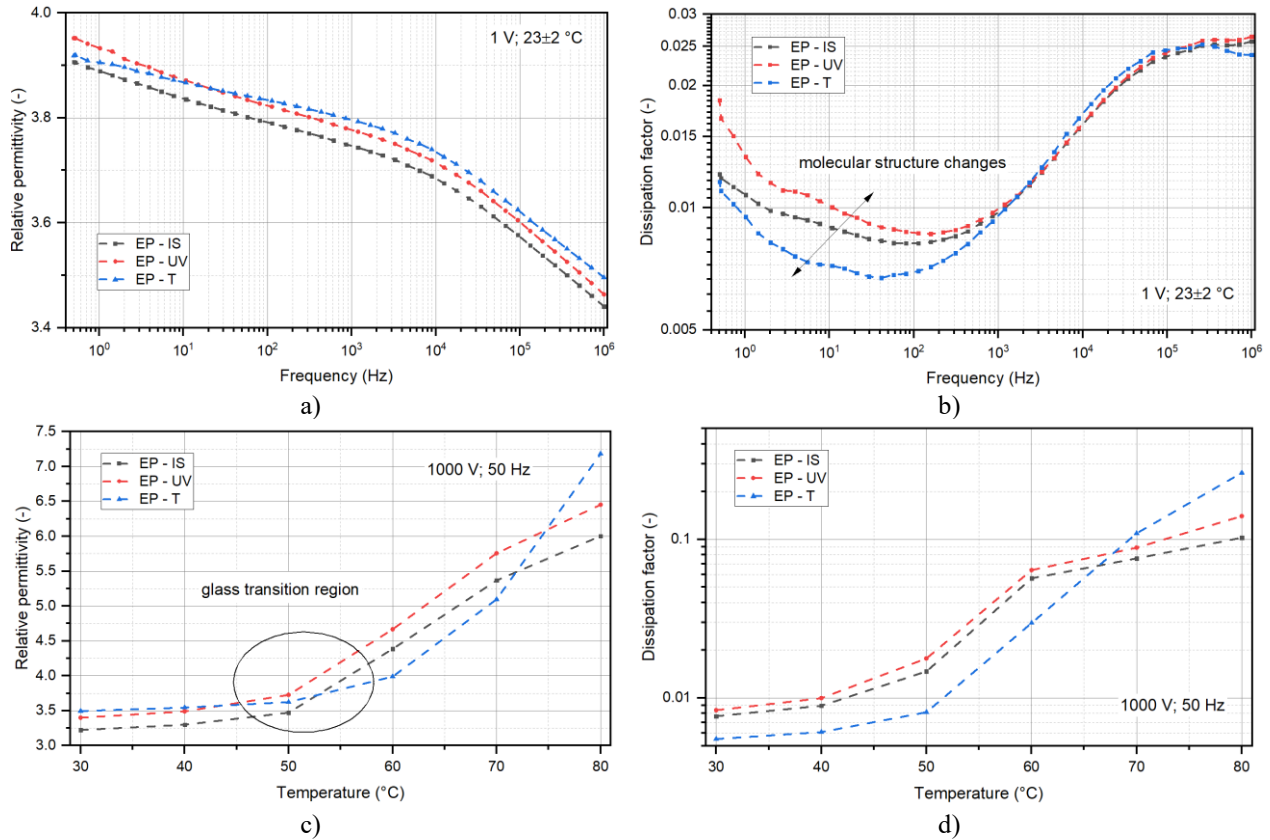

a)

b)

c)

d)

FIGURE 2. Dielectric parameters of EPs: a) frequency dependence of relative permittivity; b) frequency dependence of dissipation factor; c) temperature dependence of relative permittivity; d) temperature dependence of dissipation factor.

From the measurement results is visible, that the changes of relative permittivity before and after exposures are not significant in whole frequency range. More significant changes are observed in the loss factor. Here a decrease in dielectric loss is visible in the region of lower temperatures and frequencies. This is mainly caused by the rearrangement of the molecular structure of epoxy resin and it can be most likely attributed to the resonance of the chains or segments of molecular structure [9]. The temperature dependence of both investigated parameters shows that the thermal exposure also affects their trends. A different behavior can be observed near the assumed glass transition region (according to our earlier study [10] where $Tg \approx 47$ °C was estimated by DSC measurements) and therefore these changes can be attributed to changes in the internal structure of the material (most likely scission of molecular chains and polar group generation). These molecular changes can lead to changes in the mobility of the polymer chains, which brings with it changes in the glass transition of material together with the changes in the dielectric behavior. Looking at the results representing the changes in dielectric parameters upon UV-B exposure, only a slight effect of radiation on their deterioration is observed, but following the trend of the resin in the as-delivered state.

Volume Resistivity and Space Charge Measurement

Another of the basic dielectric parameters is volume resistivity. This parameter characterizes the behavior of dielectric material in interaction with a DC electric field. The measurements were performed with a precision electrometer (6517A, Keithley) with a three-electrode system (8009 Resistivity Test Fixture, Keithley) at an applied DC voltage of 1000 V and an ambient temperature of 23±2°C. In addition to the volume resistivity, the space charge at an applied electric field strength of 15 kV/mm [11] was also characterized. For this purpose, a device operating on

the principle of pulsed electroacoustic wave PEA (Techimp) was used. The results of the values of the volume resistivity (at a field ≤ 1 kV/mm, 3600 s), the average of maximal electric field strength and total maximal electric field strength inside the dielectric material (at a stress field 15 kV/mm) are shown in Table 1. Fig. 3 shows the patterning of the space charge density in the sample 120 s before and 120 s after disconnection from the voltage source (charging time 7200 s).

TABLE 1. Dielectric parameters of EPs at DC voltage application.

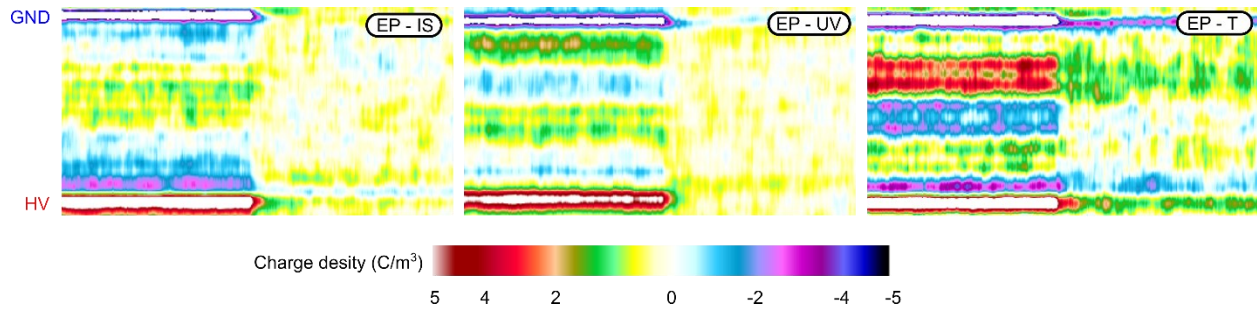| Material	Volume resistivity (Ω·cm)	Average maximal field strength (kV/mm)	Total maximal field strength (kV/mm)
EP – IS	$1.3 \cdot 10^{15} \pm 2.5 \cdot 10^{14}$	34 ± 15	68
EP – UV	$9.3 \cdot 10^{14} \pm 4.9 \cdot 10^{13}$	26 ± 10	48
EP – T	$9.1 \cdot 10^{14} \pm 8.1 \cdot 10^{13}$	33 ± 10	73

FIGURE 3. Space charge pattern profiles for different aging factors.

From the results shown in Table 2, there is a significant dispersion of the electrical field strength with polarization time, which is also visible from the space charge pattern diagram (Fig. 3). The different behavior for different types of degradation is also evident from this representation. For temperature aged material, the region inside the dielectric is also highly stressed, which is mainly visible from the pattern diagram, while it can be seen that for UV-B aged material the charge distribution inside the sample is lower and opposite. Thus, there is an assumption that charge carriers with opposite polarity are trapped during poling [12] in UV-B and thermally aged samples. For UV-B aged material this fact results in a reduction in local stress maximum compared to thermally aged material and also for material in the as-delivered state, where a higher charge density is seen primarily near the electrodes while increasing in time [13]. Furthermore, it is also necessary to consider the fact, that the resin used for this experiment is designed primarily for the encapsulation of low voltage components and higher voltage exposure can cause unusual behavior in terms of space charge formation.

The pattern diagram represented in Fig. 3 also shows that after disconnection from the source, the thermally aged material caused significant charge trapping in its structure, that symbolizing a higher level of degradation [14] in comparison with other tested materials. The results of the volume resistivity measurements show that at lower electric field levels the degradation of the material does not significantly occur.

Tensile Strength Measurement

Tensile strength measurements very often provide information on the state of degradation of the material as it is a destructive test. Tensile tests were performed on universal testing machine (LabTest 3.030, LaborTech) at room temperature (23±2 °C). It is evident from the measurements made that there is significant mechanical degradation in terms of tensile properties caused by thermo-oxidation [15] and photooxidation [16]. This is presented by a significant decrease in tensile strength. Specifically, the following evolution of tensile strengths is observed: (i) EP – IS: 44±7 MPa, (ii) EP – UV: 38±6 MPa, and (iii) EP – T: 19±5 MPa. This means that the tensile strength dropped by more than half due to thermal exposure, which could affect the reliability of the entire encapsulated component in terms of mechanical protection functionality.

Fourier-transform infrared spectroscopy was used to detect degradation caused by selected exposures. The infrared spectra were measured by a Nicolet 380 spectrometer (Thermo Scientific) together in Attenuated total reflection (ATR - using diamond crystal) and transmission mode with a resolution of 4 cm^{-1} in the frequency range of 4000–400 cm^{-1} (in Fig. 4 shown from 800 cm^{-1}). A pellet was prepared for the transmission measurement when approximately 3 mg of sample was well mixed into 180 mg of fine alkali halide (KBr) powder and then finely pulverized and put into a pellet-forming die. Afterward, the pellet was immediately put into the sample holder, and FTIR spectra were recorded. Measured spectra for both methods are in the figures below.
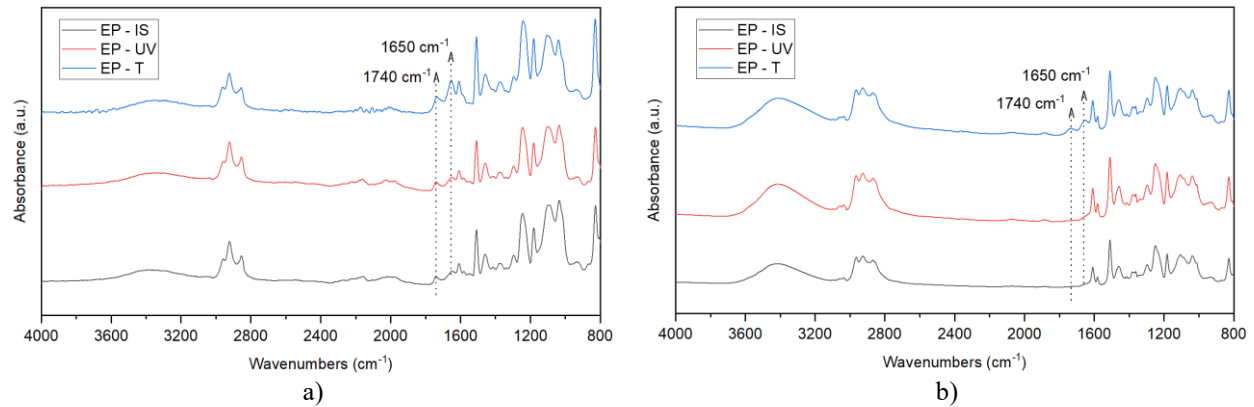

FIGURE 4. Spectral analyses of EPs: a) transmission measurement; b) ATR measurement

Figure 4 shows that an additional spectral band characterizes measured spectra of aged samples at 1740 cm^{-1} and 1650 cm^{-1} wavenumbers. According to [17] spectral band at 1740 cm^{-1} represents the vibration of the carbonyl group peak ($vC=O$) releasing as a result of an oxidation process. Similarly, the spectral peak of amides at 1650-1670 cm^{-1} could be visible as the photooxidation results [18]. These phenomena were accompanied by typical discoloration of the samples: (i) EP – T: browning, and (ii) EP – UV: yellowing. The increased presence of the above groups may also affect the space charge distribution and other material properties [19].

CONCLUSIONS

In this study, experiments on accelerated aging by extreme effects (temperature and UV-B radiation) were performed. The experimental results show the following facts. The investigations carried out revealed that there are insignificant changes in the behavior of the dielectric parameters during low-voltage tests. At higher electric field strengths, a change in material behavior in terms of space charge generation and distribution and charge dynamics is evident. In terms of mechanical properties, the tensile strength of the thermally aged material decreases by more than half. Using FTIR it was verified that thermo- and photo-oxidation occurred during exposure.

ACKNOWLEDGMENTS

REFERENCES

1. S. K. Bobade, *et. al*. Polym. Plast. Technol. Eng, **55**, 1863-1896 (2016).
2. J. A. Gannon. "High performance polymers: Their origin and development," in *History and Development of Epoxy Resins*, edited by G. S. Kirshenbaum (Springer, Dordrecht, 1986), pp. 299–307.
3. S. Nikafshar, *et. al*. Prog. Org. Coat. **151**, 106108 (2021).

4. H. Maljaee, *et. al.* Compos. B Eng. **113**,152–163 (2017).
5. M. Frigione, *et. al.* J. Polym. Eng. **21**, 23–51 (2001).
6. L. S. Lee, "4 - Rehabilitation and service life estimation of bridge superstructures" in *Service Life Estimation and Extension of Civil Engineering Structures*, edited by M. Karbhari and L. S. S. Lee (Woodhead Publishing, Oxford, 2011), pp. 117-142
7. H. Sukanto, *et. al.* Open. Eng. **11**, 797–814 (2021).
8. I. A. Saeedi, *et. al.* Polymers **11**, 1271 (2021).
9. M. Nedjar, *et. al*. J. Appl. Polym. Sci. **102**, 4728–4733 (2006).
10. J. Hornak, *et. al.* AIP Conference Proceedings **2411**, 050005 (2021).
11. J. Naveen, *et. al.* Energies **14**, 8005 (2021).
12. C. Cañadas, *et. al.* J. Phys. D: Appl. Phys. **52**, 155301 (2019).
13. O. Gallot-Lavallée, *et. al.* J. Phys. D: Appl. Phys. **38**, 2017–2025 (2005).
14. X. Jiang, *et. al.* Polymers, **12**, 634 (2020).
15. M. S. Lin and Ch. Ch. Chiu, Polym. Degrad. Stab. **71**, 327-329 (2001).
16. S. Nikafshar, *et. al.* Materials **10**, 180 (2017).
17. A. E. Krauklis and A. T. Echtermeyer, Polymers **10**, 1017 (2018).
18. K. A. M. dos Santos, *et. al.* Polym. Degrad. Stab. **90**, 34-43 (2005).
19. C. Wang, *et. al.* J. Electr. Eng. Technol. **13**, 2412-2420 (2018).